Coordination Chemistry Reviews, 119 (1992) 1–28
Elsevier Science Publishers B.V., Amsterdam

Europium complexes with organic ligands containing oxygen as donor atom. Calculation of crystal-field and scalar strength parameters for C_{3v}, D_3 and D_{3d} symmetries

M.C.F. Cunha, H.F. Brito, L.B. Zinner and G. Vicentini*
Instituto de Química, Universidade de São Paulo, Caixa Postal 20.780, CEP 01498, São Paulo (Brazil)
A.B. Nascimento
Departamento de Química, Universidade Federal da Paraíba, João Pessoa, CEP 58000, Paraíba (Brazil)

(Received 23 March 1991)

CONTENTS

ABBREVIATIONS

MeCN	acetonitrile
BCO_h	bicapped octahedral
BCTP	bicapped trigonal prism
dmp	2,2-dimethoxypropane
DMA	*N*,*N*-dimethylacetamide
DDPA	*N*,*N*-dimethyl-diphenylphosphinamide
DMSO	dimethylsulphoxide
DPPA	diphenylphosphinamide
DTMSO	1,4-dithiane monosulphoxide
HMPA	hexamethylphosphoramide

*To whom correspondence should be addressed.

IR	infrared
MCO_h	monocapped octahedral
MCTP	monocapped trigonal prism
$PhNO_2$	nitrobenzene
$MeNO_2$	nitromethane
O_h	octahedral
2-picNO	2-picoline-*N*-oxide
3-picNO	3-picoline-*N*-oxide
4-picNO	4-picoline-*N*-oxide
pyzNO	pyrazine-*N*-oxide
pyO	pyridine-*N*-oxide
TeCTP	tetracapped trigonal prism
TMSO	tetramethylene sulphoxide
TMU	tetramethylurea
TSO	thioxane oxide
TCTP	tricapped trigonal prism
teof	triethyl orthoformate
TAP	trigonal antiprism
TP	trigonal prism

A. INTRODUCTION

Lanthanide coordination compounds containing oxygen donor organic ligands have been studied for about 30 years in our laboratories at the University of São Paulo. A large number of ligands has been used in reactions with salts containing different inorganic and organic counter anions, with low coordination ability and with coordinating properties. The scope of the study is to contribute to the coordination chemistry of this series of elements, taking into account the synthesis, characterization and properties of the complexes in order to detect the nature and mode of bonding of the ligands, coordination or not of the anions and mode of coordination when pertinent and the most frequent coordination numbers. Spectroscopic properties and parameters, thermoanalytical behaviour and structural aspects have also been explored.

Only europium(III) complexes in the trigonal symmetries (C_{3v}, D_3, D_{3d}) synthesized in our laboratories are included. In all cases, the study is based on the emission spectrum at 77 K of the complexes in the visible region, using solid samples. The $^5D_0 \rightarrow {}^7F_{0,1,2}$ transitions were explored to suggest symmetries and to determine the energies of the different levels in order to calculate the crystal-field and scalar strength parameters and to try to correlate energies and parameters. Crystal-field calculations using the tensor operator technique [1], operator equivalent [2–6] and Wigner coefficients [7] methods were made. The scalar parameters, N_v [8] and S [9–13] were determined. The calculations involved 47 compounds.

Before starting the spectroscopic studies, a few items devoted to the description of the synthesis, conductance data, and IR spectra of the complexes will be included. The two latter items, together with the europium spectral study, are important for the conclusions concerning attribution of symmetry of the species.

B. SYNTHESIS, CONDUCTANCE DATA, IR SPECTRA, SYMMETRIES AND GEOMETRIES OF THE COMPLEXES

Table 1 contains a summary of data concerning the synthesis and properties of the europium complexes. It is organized in alphabetical order of the ligands and in chronological date of publication in each ligand. Preparation procedures were performed using the respective hydrated salts, except for some methanesulphonates where the anhydrous salt was used. In the case of recently prepared hexafluorophosphates, a concentrated aqueous solution was employed. In the remaining cases organic solvents (indicated in Table 1) or the ligand were employed as reaction medium. Triethyl orthoformate and 2,2-dimethoxypropane were used as dehydrating agents and/or as precipitating agents.

Conductance measurements were performed at 25°C, generally using millimolar solutions in the solvents nitromethane and acetonitrile, but in some cases methanol or nitrobenzene were employed. The existence of ion pairs was detected in some cases.

IR spectra, using Nujol mulls between KBr plates for the complexes or films of the liquid ligands, were recorded in order to detect the coordination modes of the ligands and/or anions. Shifts of the $\nu X \rightarrow 0$ (X = C, N, P, S) to lower frequencies in relation to the free ligand were found, indicating coordination through the oxygen. Table 1 contains only the frequencies attributed to the anions.

The apparent coordination numbers, symmetries and geometries were attributed on the basis of all the data obtained, but also considering the emission spectra of the compounds.

The microcrystalline nature and the hygroscopy of the majority of the complexes prepared are responsible for the lack of structural studies and for the necessity of using indirect methods for the attributions made.

Considerations about the essentially ionic nature of the bonds between Ln^{3+} and ligands were obtained from the neodymium absorption spectra (not included in this review), based on the parameters: nephelauxetic (β), covalent factors ($b^{1/2}$) [14] and Sinha's parameter (δ) [15].

C. CRYSTAL-FIELD CALCULATIONS

An important characteristic of the lanthanide elements is the small spatial extension of the 4f shell. Thus, even in the compounds, the 4f electrons, which belong to inner orbitals, are shielded from ligand interactions by the closed 5s 5p external

TABLE 1

Synthesis and properties of the europium complexes

Complex	Solvent	Conductance	IR (anion) (cm^{-1})	CN (app.)	Sym.	Geom.	Ref.
1 $Eu(ClO_4)_3 \cdot 7DMA$	DMA	–	$\nu_3 = 1100$, $\nu_4 = 740$	7	C_{3v}	MCTP	16,23
2 $Eu(NO_3)_3 \cdot 3DMA$	DMA	Non-electrolyte ($MeNO_2$)	$\nu_4 = 1455$, $\nu_1 = 1300$, $\nu_2 = 1032$, $\nu_6 = 817$, $\nu_3 = 737$	9	C_{3v}	MCTP	17,23
3 $Eu(CH_3COO)_3 \cdot DMA$	DMA	–	–	7	D_3	TP	18,23
4 $EuCl_3 \cdot 3.5DMA$	DMA	Non-electrolyte ($MeNO_2$)	–	7	D_3 (dimeric)	TP	19,23
5 $Eu(NCS)_3 \cdot 4DMA$	DMA	Non-electrolyte	$\nu C{\equiv}N = 2070$, $\nu CS = 750$	7	C_{3v}	MCTP	20,23
6 $Eu(PF_6)_3 \cdot 7DMA$	H_2O, teof	1:3 ($MeNO_2$, MeCN)	$\nu_3 = 835$, $\nu_4 = 558$	7	C_{3v}	MCTP	21,23
7 $EuI_3 \cdot 6DMA \cdot 4H_2O$	Acetone, teof of dmp	1:3 (MeCN)	–	10	C_{3v}	TP	22,23
8 $Eu(F_3C{-}SO_3)_3 \cdot 7.5DMSO$	teof	1:2 (ion pairs) ($MeNO_2$) (Methanol)	$\nu_{as}SO_3 = 1260$, $\nu_sSO_3 = 1025$	8	D_{3d}	–	24
9 $Eu(NCS)_3 \cdot 4DDPA$	Ethanol	Non-electrolyte ($MeNO_2$, MeCN)	$\nu C{\equiv}N = 2065$, 2058 $\delta NCS = 495$	7	C_{3v}	MCTP or MCO_h	25,26
10 $EuCl_3 \cdot 4DPPA$	Ethanol	–	–	7	C_{3v}	MCO_h	27,29,30
11 $EuBr_3 \cdot 5DPPA$	teof	1:1 ($MeNO_2$) 1:2 (Methanol)	–	8	C_{3v}	BCTP	28,29,30
12 $Eu(F_3C{-}SO_3)_3 \cdot 5DPPA$	Acetone, teof, dmp	1:1 ($MeNO_2$) 1:2 (MeCN)	$\nu_{as}SO_3$ = several bands $\nu_sSO_3 = 1032$, 1020	6	C_{3v} (distorted)	TAP	31
13 $EuCl_3 \cdot 3DPPM$	Ethanol, dmp	Non-electrolyte ($MeNO_2$)	–	6	C_{3v}	O_h	32,33

14	$EuBr_3 \cdot 3DPPM$	teof	Non-electrolyte ($MeNO_2$, MeCN)	–	6	C_{3v}	TP or O_h	32,33
15	$Eu(PF_6)_3 \cdot 7.5DTMSO$	Ethanol	1:3 ($MeNO_2$, MeCN)	$\nu_3 = 832$, $\nu_4 = 506$	8	D_{3d}	BCO_h (dimeric)	34
16	$Eu(H_3C{-}SO_3)_3 \cdot 2HMPA$	dmp	Non-electrolyte (methanol)	$\nu_{as} = SO_3 = 1265, 1245, 1230$ $\nu_s SO_3 = 1160, 1120, 1110$	8	C_{3v}	BCTP	35
17	$Eu(ClO_4)_3 \cdot 7(2\text{-picNO}) \cdot 3H_2O$	*n*-Butanol	1:3 ($MeNO_2$, MeCN)	$\nu_3 = 1093$, $\nu_4 = 625$	7	C_{3v}	MCTP	36,39
18	$EuCl_3 \cdot 3(2\text{-picNO}) \cdot 2H_2O$	Ethanol, teof	1:1 (methanol)	–	8	C_{3v}	BCTP	37,39
19	$Eu(NCS)_3 \cdot 3(2\text{-picNO})$	*n*-Butanol	Non-electrolyte (MeCN)	$\nu C{\equiv}N = 2040$, $\delta NCS = 470$	6	C_{3v}	TP	38,39
20	$Eu(NCS)_3 \cdot 4(2\text{-picNO})$	*n*-Butanol	Non-electrolyte (MeCN)	$\nu C{\equiv}N = 2040$, $\delta NCS = 470$	7	C_{3v}	MCTP	38,39
21	$Eu(ReO_4)_3 \cdot 5(2\text{-picNO})$	*n*-Butanol	–	$\nu_3 = 910, 870$, $\nu_4 = 290$	8	C_{3v}	BCTP	40
22	$Eu(ReO_4)_3 \cdot 3(2\text{-picNO})$	MeCN	–	$\nu_3 = 897, 860$, $\nu_4 = 290$	6	C_{3v}	TP	40
23	$Eu(H_3C{-}SO_3)_3 \cdot 2(3\text{-picNO})$	Acetone, teof or dmp	Non-electrolyte (Methanol)	$\nu_{as} SO_3$ = several bands $\nu_s SO_3$ = several bands	8	C_{3v}	BCTP	41
24	$Eu(NCS)_3 \cdot 3.5(3\text{-picNO})$	teof	Non-electrolyte ($MeNO_2$, MeCN)	$\nu CN = 2040$, $\nu CS = 798$, $\delta NCS = 480$	–	C_{3v}	–	42
25	$Eu(NCS)_3 \cdot 3.5(4\text{-picNO})$	teof	Non-electrolyte ($MeNO_2$)	$\nu C{\equiv}N = 2060$, $\delta NCS = 470$	–	C_{3v}	–	43
26	$Eu(H_3C{-}SO_3)_3 \cdot 2(4\text{-picNO})$	Methanol, teof	Non-electrolyte (methanol)	ν_{as} = several bands $\nu_s = 1052$	8	C_{3v}	–	44
27	$Eu(ClO_4)_3 \cdot 8pyzNO$	Ethanol, dmp	1:3 (MeCN) 1:2 ($MeNO_2$) (ion pairs)	$\nu_3 = 1088$, $\nu_4 = 618$	8	D_{3d}	BCO_h	45,48
28	$Eu(PF_6)_3 \cdot 8pyzNO$	Water, ethanol, teof	1:3 (MeCN) ($MeNO_2$)	$\nu_3 = 825$, $\nu_4 = 560$	8	D_{3d}	BCO_h	46,48

TABLE 1 (*continued*)

Complex	Solvent	Conductance	IR (anion) (cm^{-1})	CN (app.)	Sym.	Geom.	Ref.
29 $Eu(NCS)_3 \cdot 4pyzNO$	teof	Non-electrolyte (MeCN)	$\nu C{\equiv}N = 2035$, $\delta NCS = 475$	7	C_{3v}	MCTP	47,48
30 $Eu(F_3C{-}SO_3)_3 \cdot 6pyzNO \cdot 3H_2O$	teof	1:2 (MeCN) (ion pairs)	$\nu_{as}SO_3 = 1259$ $\nu_sSO_3 = 1033$	9	C_{3v}	TCTP	49
31 $Eu(H_3C{-}SO_3)_3 \cdot 2pyO$	Methanol, teof	Non-electrolyte (methanol)	$\nu_{as}SO_3$ = several bands $\nu_sSO_3 = 1066, 1059$	8	C_{3v}	–	50
32 $Eu(ClO_4)_3 \cdot 8TMSO$	Ethanol	1:3 ($MeNO_2$)	$\nu_3 = 1083$, $\nu_4 = 621$	8	D_{3d}	BCO_h	51,59
33 $Eu(NCS)_3 \cdot 4TMSO$	*n*-Butanol	Non-electrolyte ($MeNO_2$)	$\nu C{\equiv}N = 2041$, $\delta NCS = 481, 475$	7	C_{3v}	MCTP	52,59
34 $EuCl_3 \cdot 3TMSO$	Ethanol, teof	Non-electrolyte (MeCN)	–	6	C_{3v}	TP	53,59
35 $Eu(PF_6)_3 \cdot 7.5TMSO$	Water, teof	1:3 ($MeNO_2$, MeCN)	$\nu_3 = 983$, $\nu_4 = 560$	8	D_{3d}	BCO_h (dimeric)	54,59
36 $EuBr_3 \cdot 7TMSO$	dmp	1:1 ($MeNO_2$) 1:2 (methanol)	–	8	D_{3d}	BCO_h	55,59
37 $Eu(ReO_4)_3 \cdot 7.5TMSO$	Methanol	1:1 ($MeNO_2$, MeCN) (ion pairs)	$\nu_3 = 980$	8	D_{3d}	BCO_h (dimeric)	56
38 $EuI_3 \cdot 7.5TMSO$	Acetone	1:3 ($MeNO_2$, MeCN)	–	8	D_{3d}	BCO_h (dimeric)	57
39 $Eu(F_3C{-}SO_3)_3 \cdot 7.5TMSO$	teof	1:2 ($MeNO_2$, MeCN) (ion pairs)	$\nu_{as}SO_3 = 1275$, $\nu_sSO_3 = 1030$	8	D_{3d}	BCO_h (dimeric)	58
40 $EuCl_3 \cdot 3TMU$	TMU	Non-electrolyte ($MeNO_2$)	–	6	D_3	–	60,62

41	$Eu(NCS)_3 \cdot 3.5TMU$	TMU	Non-electrolyte ($MeNO_2$, $PhNO_2$)	$\nu C{\equiv}N = 2070, 2040$ $\delta NCS = 482$	–	C_{3v}	–	61,62
42	$EuCl_3 \cdot 4.5TSO$	Ethanol	1:1 (methanol)	–	8	C_{3v}	BCTP	63,68
43	$Eu(NCS)_3 \cdot 5TSO$	Ethanol	Non-electrolyte ($MeNO_2$)	$\nu C{\equiv}N = 2060, 2030$ $\nu CS = 764$, $\delta NCS = 469$	8	C_{3v}	BCTP	64,68
44	$Eu(ClO_4)_3 \cdot 7.5TSO$	Ethanol	1:2 ($MeNO_2$) (ion pairs)	$\nu_3 = 1087$, $\nu_4 = 619$	8	D_{3d}	BCO_h (dimeric)	65,68
45	$Eu(PF_6)_3 \cdot 7.5TSO$	Ethanol	1:3 ($MeNO_2$, MeCN)	$\nu_3 = 836$, $\nu_4 = 558$	8	D_{3d}	BCO_h (dimeric)	66,68
46	$EuI_3 \cdot 7.5TSO$	Acetone	1:2 (MeCN, methanol) 1:1 ($MeNO_2$) (ion pairs)	–	8	D_{3d}	BCO_h (dimeric)	67,68
47	$Eu(F_3C{-}SO_3)_3 \cdot 7.5TSO$	teof	1:1 ($MeNO_2$) (ion pairs)	$\nu_{as}SO_3 = 1240$, $\nu_sSO_3 = 1028$	8	D_{3d}	BCO_h (dimeric)	69

orbitals. In particular, the spectra of the compound containing 4f electrons in the solid state retain similar atomic-like properties, which is of great help in the interpretation of their level structure. On the other hand, the small crystal-field perturbation can be used to investigate the surroundings of the ion, which then acts as a local probe.

The free ions present a field-free spherical symmetry, which is perturbed by the inhomogeneous field generated by the electrical charge distribution due to the ligands in the crystals. The crystal-field interaction partially removes the degeneracy of the free ion J states into a number of M_J levels that are dependent on the site symmetry occupied by the ion.

Knowledge of the crystal-field symmetry is very important in the interpretation of optical spectra. The crystal-field levels are, according to group theory, associated with irreducible representation (γ_{Γ_n}) belonging to the symmetry group under consideration [1,70–76].

To determine the crystal-field parameters, three methods were utilized: the tensor operator technique [77], the operator equivalent method [3] and the Wigner coefficients method [7].

(i) The tensor operator technique

A general approach considers the potential energy, $V(r)$, of an electron of a central ion, where r is the radius associated with an f electron. The environment is represented by a classical charge distribution $\rho(R)$, where R is the radius associated with a general point in that environment, then

$$V(r) = -\int \frac{e\rho(R)}{|R-r|}\,\mathrm{d}r \tag{1}$$

According to the parametric approach, it is convenient to write this potential in terms of B_q^k parameters with the Wybourne formalism [1].

The sum over the i electrons may be written as

$$V_{\mathrm{CF}} = \sum_{k,q,i} B_q^k C_q^k(\theta_i \phi_i) \tag{2}$$

where B_q^k (s) are the crystal-field parameters (radial integrals)

$$B_q^k = -e\int (-1)^q \rho(R) C^k{}_{-q}(\theta\phi)\frac{r_<^k}{r_>^{k+1}}\,\mathrm{d}r \tag{3}$$

and C_q^k are tensor operators of rank k for the angular part of the crystal-field interaction [1].

The matrix elements of this crystalline potential among coupled states having

the same J values (to retain eigenvalues) are obtained using the Racah's techniques [71,74–77].

$$\langle f^N WUSLJM_J|H_{ij}|f^N W'U'SL'J'M'_J\rangle$$
$$= \sum B^k_q \langle f^N WUSLJM_J|U^k_q|f^N W'U'SL'J'M'_J\rangle \langle l\|C^k\|l'\rangle \quad (4)$$

where

$$\langle l\|C^k\|l'\rangle = (-1)^l[(2l+1)(2l'+1)]^{1/2}\begin{pmatrix} l & k & l' \\ 0 & 0 & 0\end{pmatrix}$$

$$\langle f^N WUSLJM_J|U^k_q|f^N W'U'SL'J'M'_J\rangle$$
$$= (-1)^{J-M_J}\begin{pmatrix} J & k & J' \\ -M_J & q & M_{J'}\end{pmatrix}\cdot\langle f^N WUSLJ|U^k|f^N W'U'SL'J'\rangle$$

$$\langle f^N WUSLJ|U^k|f^N W'U'SL'J'\rangle$$
$$= (-1)^{S+L'+J+k}\cdot[(2J+1)(2J'+1)]^{1/2}\cdot\begin{pmatrix} J & J' & k \\ L' & L & S\end{pmatrix}$$
$$\cdot\langle f^N WUSL\|U^k\|f^N W'U'SL'\rangle \quad (5)$$

Doubly reduced matrix elements $\langle f^N WULS\|U^k\|f^N W'U'L'S\rangle$ can be calculated and have been tabulated by Nielson and Koster [78]. WU denotes the remaining quantum numbers required to specify the states [79–81].

$\begin{pmatrix} J & k & J' \\ -M_J & q & M'_J\end{pmatrix}$ are the 3-j symbols which have been tabulated by Rotemberg and Biving and Landolt-Börnstein [82,83].

Table 2 lists, for each of the thirty-two point groups, the non vanishing B^k_q values.

The point groups are listed in sets, each of them having the same non-vanishing B^k_q. The groups within a set are indistinguishable insofar as the symmetry properties of H_{cf} are concerned. To distinguish groups within a set, the odd-parity part of the crystal-field interaction must be examined. Equally, the point groups within a set can be distinguished by their different electric-dipole selection rules [2] (see also ref. 91).

(ii) The operator-equivalent method

In the operator-equivalent method [2–5], the coupling of different free-ion levels by the crystal-field interaction is ignored and the crystal-field splitting of each $^{2S+1}L_J$ level is treated separately. Traditionally, in this method, the Hamiltonian of

TABLE 2
Non-zero B_q^k parameters for the 32 point groups

Point group	Parameters B_q^k		
	$K=2$	$K=4$	$K=6$
C_1 C_i	All (B_1^2 real)	All	All
C_2 C_s (C_{1h}) C_{2h}	B_0^2, Re B_2^2	B_0^4, B_2^4, B_4^4	B_0^6, B_2^6, B_4^6, B_6^6
D_2 C_{2v} D_{2h}	B_0^2, Re B_4^4	B_0^4, Re($B_2^4 B_4^4$)	B_0^6, Re B_2^6, Re B_4^6, Re B_6^6
C_4 S_4 C_{4h}	B_0^2	B_0^4, Re B_4^4	B_0^6, B_4^6
D_4 C_{4v} D_{2d} D_{4h}	B_0^2	B_0^4, Re B_4^4	B_0^6, Re B_4^6
C_3 S_6 (C_{3i})	B_0^2	B_0^4, Re B_3^4	B_0^6, B_3^6, B_6^6
D_3 C_{3v} D_{3d}	B_0^2	B_0^4, Re B_3^4	B_0^6, Re B_3^6, Re B_6^6
C_6, C_{3h}, C_{6h}, D_6, C_{6v}, D_{3h}, D_{6h}	B_0^2	B_0^4	B_0^6, Re B_6^6
T, T_d, T_h, O, O_h	–	B_0^4, Re B_4^4	B_0^6, Re B_4^6

the crystalline field is written as

$$H_{CF} = \sum_{k,q} A_k^q \sum_i V_k^q(r_i) \tag{6}$$

Where A_k^q are crystal-field components, and the $V_k^q(r_i)$ are polynomials in the x, y and z coordinates of the ith electron. These polynomials are tabulated for $2 \leqslant k \leqslant 6$ and $|q| \leqslant k$ in refs. 3 and 84.

In the operator-equivalent method, one is concerned with matrix elements of eqn. (6) within a given free-ion state denoted by $^{2S+1}L_J$. The V_k^q polynomials may

be replaced

$$\sum V_k^q(r_i) \rightarrow \theta_j^k \langle r^k \rangle O_k^q \tag{7}$$

Where θ_j^k ($=\alpha_j$ for $k=2$, β_j for $k=4$ and γ_j for $k=6$) are the operator-equivalent factors and the O_k^q are the Hermitian operator equivalents [84].

The point charge model used in this work is based on

$$B_k^q = A_k^q \langle r^k \rangle \tag{8}$$

The exact forms of the A_k^q parameters are given in ref. 85.

(iii) The Wigner coefficient method

In the Wigner coefficient method, the potential of the crystal-field is written as

$$H_{CF} = \sum_{k,q} \langle A^{2S+1}L_J \| U^k \| A^{2S+1}L_J \rangle C_{M_J q}^{JkJ'} Y_k^q \langle r^k \rangle \tag{9}$$

where $\langle A^{2S+1}L_J \| U^k \| A^{2S+1}L_J \rangle$ are the reduced matrix elements of U^k, $Y_k^q \langle r^k \rangle$ are phenomenological parameters, and $C_{M_J q}^{JkJ'}$ are the Wigner coefficients [7].

The crystal-field calculations for the three methods are performed by diagonalizing small matrices containing matrix elements of H_{CF} within a given $^{2S+1}L_J$ state.

The dimensions of these matrices are given by $(2J+1) \times (2J+1)$.

D. THE CRYSTAL-FIELD SCALAR STRENGTH PARAMETERS

To compare the magnitude of different crystal-field strengths, it is convenient to use a scalar crystal-field parameter [8] which is expressed as

$$N_v = \left[\sum \frac{4\pi}{(2k+1)} (B_q^k)^2 \right]^{1/2} \tag{10}$$

where N_v is a number which characterizes the crystal-field strength.

The parameter S was also used, as introduced by Leavitt et al. [9–13], and is invariant with the rotation axis.

$$S = \left\{ \frac{1}{3} \sum_k \frac{1}{(2k+1)} \left[(B_0^k)^2 + 2 \sum_{q>0} [(\mathrm{Re}\, B_q^k)^2 + (\mathrm{Im}\, B_q^k)^2)] \right] \right\}^{1/2} \tag{11}$$

E. EUROPIUM(III) COMPLEXES WITH TRIGONAL SYMMETRIES (C_{3v}, D_3, D_{3d})

(i) Analysis of the spectra

Strong electric dipole (ED) transitions to the $^7F_2$ crystal-field sublevels can be observed around 610 nm, due to the absence of an inversion centre symmetry in the europium sites (C_{3v}, D_3). The $^5D_0 \rightarrow {}^7F_1$ transitions induced by magnetic dipole

(MD) interactions at ca. 595 nm have strengths equal to or even higher than those of the ED transitions of D_{3d} symmetry. The intensity of the $^5D_0 \rightarrow {}^7F_0$ transition is significant in all compounds with C_{3v} symmetry whereas in others it is much weaker. The transition strength depends on the contributions from the other $^7F_{JM}$ wavefunctions to $^7F_{00}$. An intense $^5D_0 \rightarrow {}^7F_0$ transition usually indicates the presence of a strong crystal-field.

The weak $^5D_0 \rightarrow {}^7F_3$ transition is difficult to record. The very low intensity of this transition has recently been reported and is related to a small J-mixing effect (mixture of $^7F_{1,2,4}$) wavefunctions with $^7F_3$ leading to a mixed MD–ED character [70,86–89]. Our available spectroscopic equipment does not allow us to record this transition. For these reasons, the parameters with $k = 6$ were not calculated.

Following calculations, it was realised that the diagrams used for all the compounds could be summarized in two models, which are presented in Fig. 1.

Mülliken's notation was used in the diagrams to designate the J sublevels. In

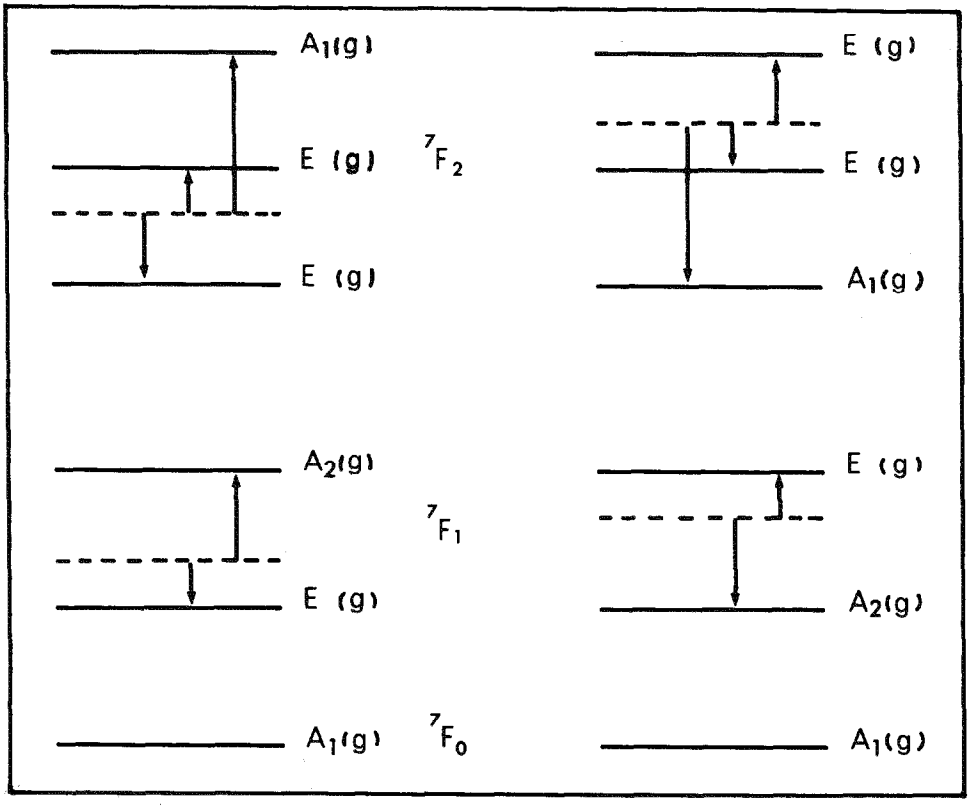

Fig. 1. Qualitative energy levels for C_{3v}, D_3 and D_{3d} symmetries.

TABLE 3

Splitting of the $^{2S+1}L_J$ ($J = 0$–6) levels in C_{3v}, D_3 and D_{3d} symmetries (for D_{3d} symmetry the character g has to be included in the irreducible representation) [90]

D_J	J						
	0	1	2	3	4	5	6
A_1	1	–	1	1	2	1	3
A_2	–	1	–	2	1	2	2
E	–	1	2	2	3	4	4

the case of the D_{3d} symmetry, the subscript g was used due to the existence of an inversion centre (Table 3).

(ii) Crystal-field parameter calculation for C_{3v}, D_3 and D_{3d} symmetries

The first term in the methods employed has $k = q = 0$ and is spherically symmetric. This term is by far the largest and is due to the Coulombic energy of a positive ion surrounded by negative charges. It corresponds to the lattice energy. It shifts all energy levels equally and does not contribute to the crystal-field splitting [86,91]. Since we are concerned only with equivalent f electrons, $k \leqslant 2l \leqslant 6$, k has to be even, therefore $k = 2, 4, 6$. The values of q are determined by the point symmetry of the $4f^N$ ion site, since the Hamiltonian must be invariant under the operations of the point symmetry group. Only the levels $^7F_{1,2}$ of europium ion were analysed, which led us to the values $k = 0, 2, 4$ and $q = 0, \pm 3$. Figures 2–7 present the energy diagrams and emission spectra of three europium compounds with C_{3v}, D_3 and D_{3d} symmetries.

The operator equivalent and tensorial method matrix elements can be found elsewhere [92,93]. For the Wigner coefficient method, the following is shown.

$$\text{For } J = 1 \qquad \begin{aligned} \langle \pm 1 | V_2^0 | \pm 1 \rangle &= -0.06308\, Y_2^0 \langle r^2 \rangle \\ \langle 0 | V_2^0 | 0 \rangle &= 0.1262\, Y_2^0 \langle r^2 \rangle \end{aligned} \tag{12}$$

The position of the crystalline field component for the $^7F_1$ manifold level of the Eu^{3+} ion is determined for second-order terms. These energy levels (eigenvalues) are obtained from the diagonalization of the 3×3 matrix (Fig. 8).

$$\text{For } J = 2 \qquad \begin{aligned} a &= \langle \pm 2 | V_4^0 | \pm 2 \rangle = -0.06608\, Y_2^0 \langle r^2 \rangle - 0.01343\, Y_4^0 \langle r^4 \rangle \\ b &= \langle \pm 1 | V_4^0 | \pm 1 \rangle = 0.03304\, Y_2^0 \langle r^2 \rangle + 0.05373\, Y_4^0 \langle r^4 \rangle \\ c &= \langle 0 | V_4^0 | 0 \rangle = 0.06608\, Y_2^0 \langle r^2 \rangle - 0.08059\, Y_4^0 \langle r^4 \rangle \\ d &= \langle \pm 2 | V_4^{\pm 3} | \mp 1 \rangle = -0.07947\, Y_4^3 \langle r^4 \rangle \end{aligned} \tag{13}$$

The fourth-order terms are obtained from analysis of the $J = 2$ level splittings

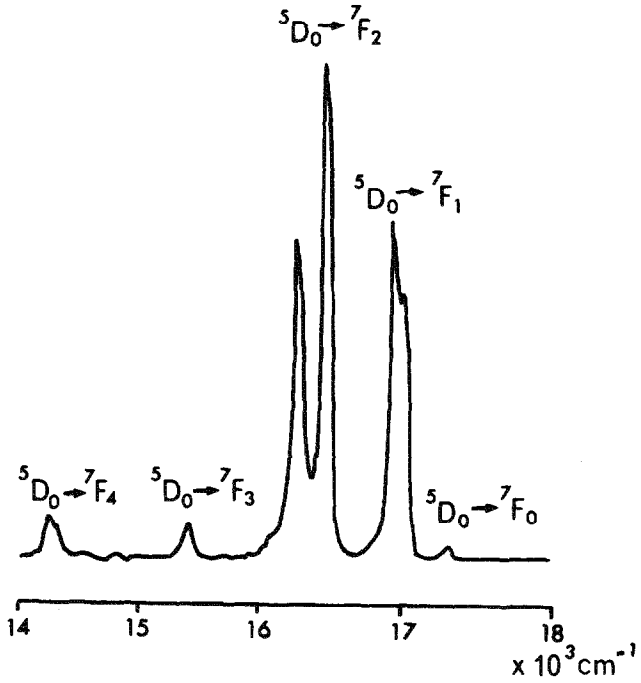

Fig. 2. Emission spectrum of the compound of formula $EuCl_3 \cdot 3TMU$ (77 K).

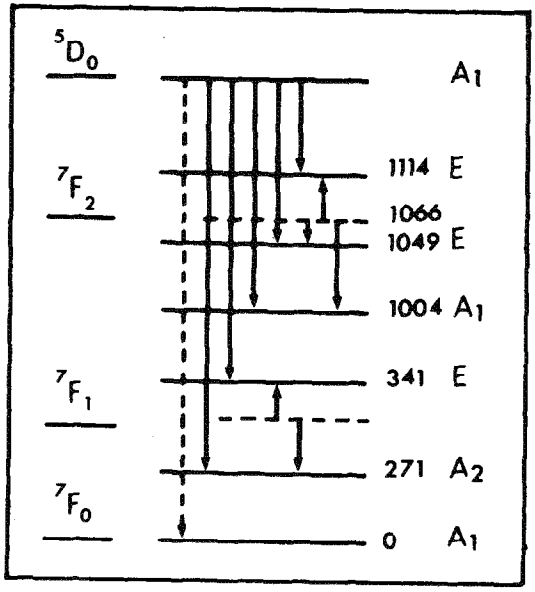

Fig. 3. Energy diagram for the compound of formula $EuCl_3 \cdot 3TMU$ (D_3 symmetry).

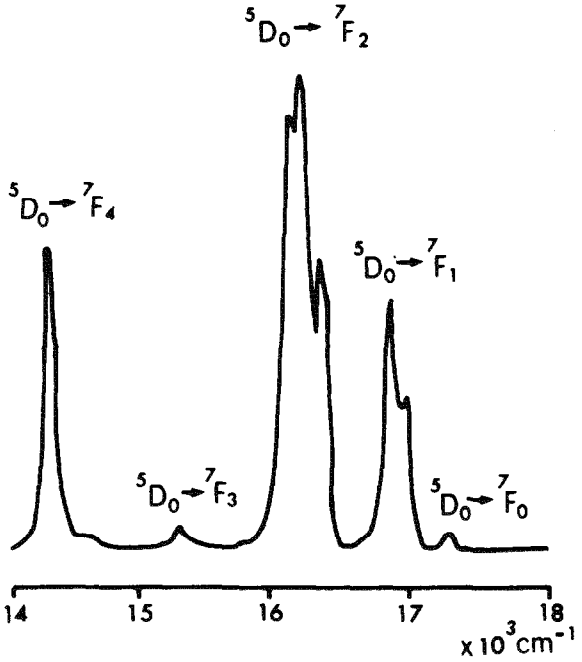

Fig. 4. Emission spectrum of the compound of formula $Eu(NCS)_3 \cdot 5TMU$ (77 K).

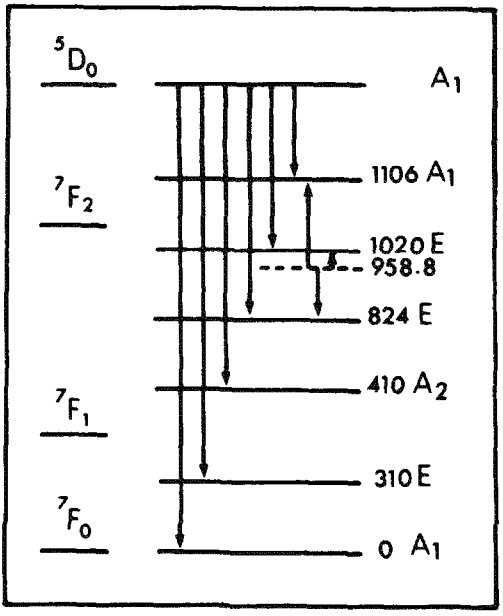

Fig. 5. Energy diagram for the compound of formula $Eu(NCS)_3 \cdot 3.5TMU$ (C_{3v} symmetry).

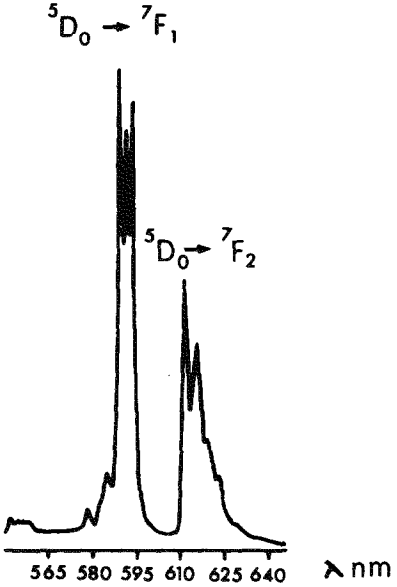

Fig. 6. Emission spectrum of the compound of formula $Eu(ClO_4)_3 \cdot 7.5TSO$.

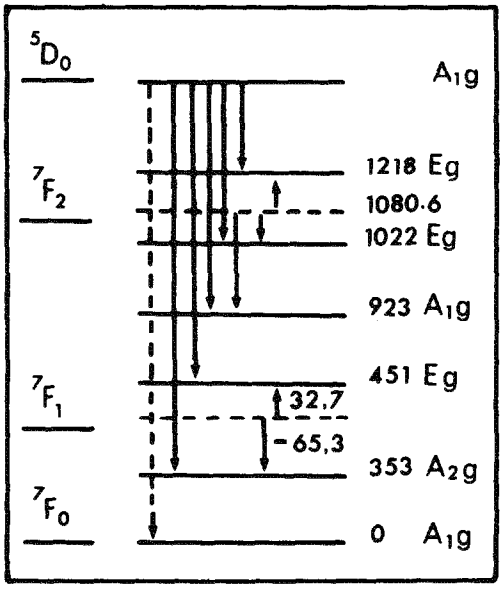

Fig. 7. Energy diagram for the compound of formula $Eu(ClO_4)_3 \cdot 7.5TSO$ (D_{3d} symmetry).

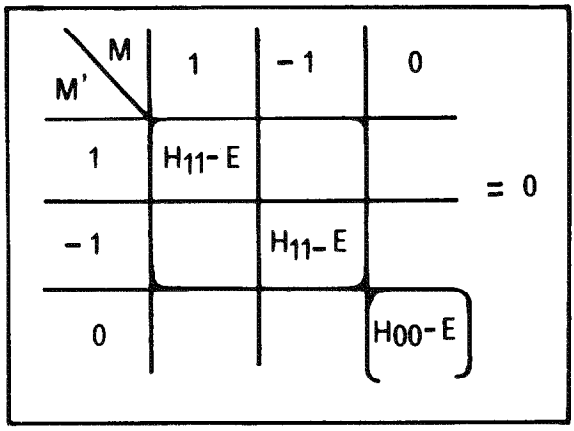

Fig. 8. Secular determinant for the $^7F_1$ manifold in C_{3v}, D_3 and D_{3d} symmetries for Eu^{3+}.

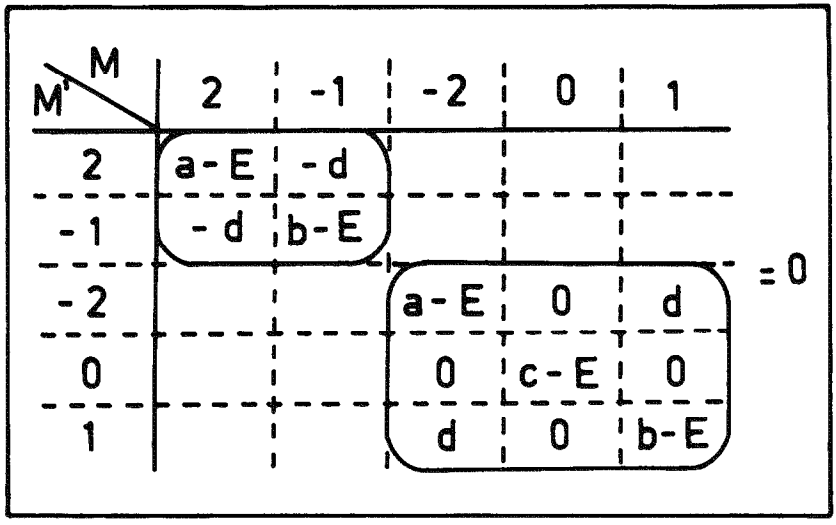

Fig. 9. Secular determinant for the $^7F_2$ manifold in C_{3v}, D_3 and D_{3d} symmetries for Eu^{3+}.

and the eigenvalues are obtained through the diagonalization of a (5 × 5) matrix (Fig. 9).

After resolving the determinants and making adequate substitutions, the parameter values presented in Table 4 were found.

It is possible to obtain the parameters in the equivalent operator formalism (B_k^q) employing the correlation tables found in ref. 1 and the corrections made by Kassman [94].

TABLE 4

Crystal-field parameters for trivalent europium complexes with C_{3v}, D_3 and D_{3d} symmetries

Complex	Methods					
	Tensorial operator			Wigner coefficient		
	B_0^2	B_0^4	B_3^4	$Y_2^0\langle r^2\rangle$	$Y_4^0\langle r^4\rangle$	$Y_4^3\langle r^4\rangle$
C_{3v} symmetry						
$Eu(ClO_4)_3 \cdot 7DMA$	−250	1229	−546	−396	1452	−646
$Eu(NO_3)_3 \cdot 3DMA$	380	−519	−409	602	−613	−483
$Eu(NCS)_3 \cdot 4DMA$	250	−1174	−740	396	−1387	−874
$Eu(PF_6)_3 \cdot 7DMA$	217	−1013	−703	343	−1197	−831
$EuI_3 \cdot 6DMA \cdot 4H_2O$	443	−1171	−697	703	−1384	−824
$Eu(NCS)_3 \cdot 4DDPA$	233	−1373	−638	370	−1622	−754
$EuCl_3 \cdot 4DPPA$	−620	217	−369	−983	256	−436
$EuBr_3 \cdot 5DPPA$	−313	1188	−767	−497	1404	−907
$Eu(F_3C{-}SO_3)_3 \cdot 5DPPA$	143	−1619	−833	227	−1913	−985
$EuCl_3 \cdot 3DPPM$	217	−1408	−970	343	−1664	−1146
$EuBr_3 \cdot 3DPPM$	−390	823	−948	−618	972	−1120
$Eu(H_3C{-}SO_3)_3 \cdot 2HMPA$	−320	1042	−703	−507	1232	−831
$Eu(ClO_4)_3 \cdot 7(2\text{-picNO}) \cdot 3H_2O$	250	−880	−501	396	−1040	−592
$EuCl_3 \cdot 3(2\text{-picNO}) \cdot 2H_2O$	313	−1180	−447	497	−1394	−528
$Eu(NCS)_3 \cdot 3(2\text{-picNO})$	243	−1341	−453	386	−1584	−535
$Eu(NCS)_3 \cdot 4(2\text{-picNO})$	227	−1481	−422	359	−1750	−499
$Eu(ReO_4)_3 \cdot 5(2\text{-picNO})$	−433	783	−862	−687	926	−1019
$Eu(ReO_4)_3 \cdot 3(2\text{-picNO})$	−417	957	−791	−661	1131	−935
D_{3d} symmetry						
$Eu(F_3C{-}SO_3)_3 \cdot 7.5DMSO$	223	−772	−739	370	−913	−873
$Eu(PF_6)_3 \cdot 7.5DTMSO$	227	−1069	−811	423	−1264	−958
$Eu(ClO_4)_3 \cdot 8pyzNO$	143	−834	−584	227	−985	−690
$Eu(PF_6)_3 \cdot 8pyzNO$	143	−779	−518	227	−920	−613
$Eu(ClO_4)_3 \cdot 7.5TMSO$	287	−1558	−898	454	−1841	−1061
$Eu(PF_6)_3 \cdot 7.5TMSO$	297	−1118	−575	470	−1322	−680
$EuBr_3 \cdot 7TMSO$	287	−1545	−702	454	−1826	−830
$Eu(ReO_4)_3 \cdot 7.5TMSO$	237	−1193	−536	375	−1410	−634
$EuI_3 \cdot 7.5TMSO$	313	−1314	−918	497	−1553	−1085
$Eu(F_3C{-}SO_3)_3 \cdot 7.5TMSO$	373	−1412	−475	592	−1669	−561
$Eu(ClO_4)_3 \cdot 7.5TSO$	−327	−1296	−1007	−518	1531	−1190
$Eu(PF_6)_3 \cdot 7.5TSO$	360	−762	−900	571	−901	−1063
$EuI_3 \cdot 7.5TSO$	407	−1316	−879	645	−1556	−1039
$Eu(F_3C{-}SO_3)_3 \cdot 7.5TSO$	200	−1040	−458	317	−1229	541
$Eu(H_3C{-}SO_3)_3 \cdot 2(3\text{-picNO})$	333	−847	−402	528	−1001	−475
$Eu(NCS)_3 \cdot 3.5(3\text{-picNO})$	143	−888	−807	227	−1049	−954
$Eu(NCS)_3 \cdot 3.5(4\text{-picNO})$	327	−1082	−706	518	−1278	−834
$Eu(H_3C{-}SO_3)_3 \cdot 2(4\text{-picNO})$	363	806	−592	576	−952	−699
$Eu(NCS)_3 \cdot 4pyzNO$	−357	1019	−505	−565	1204	−596

TABLE 4 (*continued*)

Complex	Methods					
	Tensorial operator			Wigner coefficient		
	B_0^2	B_0^4	B_3^4	$Y_2^0\langle r^2\rangle$	$Y_4^0\langle r^4\rangle$	$Y_4^3\langle r^4\rangle$
$Eu(F_3C{-}SO_3)_3 \cdot 6pyzNO \cdot 3H_2O$	−420	827	−389	−666	978	−459
$Eu(CH_3{-}SO_3)_3 \cdot 2pyO$	433	−720	−588	−690	−851	−695
$Eu(NCS)_3 \cdot 4TMSO$	240	−1097	−401	380	−1296	−474
$EuCl_3 \cdot 3TMSO$	213	−1093	−318	338	−1291	−376
$Eu(NCS)_3 \cdot 3.5TMU$	334	−1166	−1023	529	−1377	−1208
$EuCl_3 \cdot 4.5TSO$	287	−1671	−904	454	−1068	−537
$Eu(NCS)_3 \cdot 5TSO$	400	−946	−753	634	−1118	−890
D_3 symmetry						
$Eu(H_3C{-}COO)_3 \cdot DMA$	−324	984	−52	−514	1163	−62
$EuCl_3 \cdot 3.5DMA$	−460	1048	−260	−729	1238	−307
$EuCl_3 \cdot 3TMU$	−233	395	−345	−369	466	−408

Using the energy equations in the determinant, one may calculate

$$E(2,-1): E^2 \underbrace{-(a+b)}_{m} E + \underbrace{ab-d^2}_{n} = 0$$

$$E(-2,0,1) = E^3 + \underbrace{[-(a+b+c)]}_{p} E^2 + \underbrace{(ab+bc+ac-d^2)}_{q} E + \underbrace{d^2c-abc}_{r} = 0 \qquad (14)$$

where

$$m = -(a+b) = -(E_1+E_2)$$

$$n = ab - d^2 = E_1E_2$$

$$p = [-(a+b+c)] = -(E_1+E_2+E_3)$$

$$q = (ab+bc+ac-d^2) = E_1E_2 + E_2E_3 + E_1E_3 \qquad (15)$$

$$r = d^2c - abc = -(E_1E_2E_3)$$

The values of m, n, p, q, r and the roots of the equations for all the compounds are given in Table 5.

The relative strengths of the crystal-field, N_v and S, were calculated. The N_v strengths were calculated from eqn. (10) and by eqn. (15) in ref. 8. Table 6 lists the parameters for the compounds on the $^7F_{1,2}$ manifolds.

Very good correlation coefficients were obtained for the three symmetries under investigation when the scalar parameters N_v and S were plotted versus ΔE for the magnetic dipole allowed transitions $^5D_0 \rightarrow {}^7F_1$.

TABLE 5

Energy levels of $^7F_1$ and $^7F_2$ manifolds and cubic quadratic coefficients of the Eu^{3+} compounds

Compound	Level									
	$^7F_1$		$^7F_2$							
	E_1	E_2	E_1	E_2	E_3	m	n	p	$q \times 10^{-1}$	$r \times 10^{-3}$
C_{3v} symmetry										
$Eu(ClO_4)_3 \cdot 7DMA$	−50.0	25.0	94.8	−23.2	−143.2	−71.6	−2199	71.6	−1245	−314.9
$Eu(NO_3)_3 \cdot 3DMA$	76.0	−38.0	17.2	−61.8	89.2	44.6	−1063	−44.6	−504.1	94.8
$Eu(NCS)_3 \cdot 4DMA$	50.0	−25.0	40.0	−109.0	138.0	69.0	−4360	−69.0	−1338	601.7
$Eu(PF_6)_3 \cdot 7DMA$	43.4	−21.6	40.2	−99.8	119.2	59.6	−4012	−59.6	−1112	478.2
$EuI_3 \cdot 6DMA \cdot 4H_2O$	88.6	−44.4	27.0	−106.0	158.0	79.0	−2862	−79.0	−1534	452.2
$Eu(NCS)_3 \cdot 4DDPA$	46.6	−23.4	31.2	−108.8	155.2	77.6	−3395	−77.6	−1544	526.8
$EuCl_3 \cdot 4DPPA$	−124.0	62.0	74.4	−31.6	−85.6	−42.8	−2351	42.8	−601.4	−201.2
$EuBr_3 \cdot 5DPPA$	−62.6	31.4	112.0	−39.0	−146.0	−73.0	−4368	73.0	−1503	−637.7
$Eu(F_3C—SO_3)_3 \cdot 5DPPA$	28.6	−14.4	52.2	−136.8	169.2	84.6	−7141	−84.6	−2146	1208
$EuCl_3 \cdot 3DPPM$	43.3	−21.7	59.8	−138.2	156.8	78.4	−8264	−78.4	−2056	1295
$EuBr_3 \cdot 3DPPM$	−78.0	39.0	118.8	−59.2	−119.2	−59.6	−7033	59.6	−1414	−838.3
$Eu(H_3C—SO_3)_3 \cdot 2HMPA$	−64.0	32.0	101.2	−34.8	−132.8	−66.4	−3522	66.4	−1234	−467.7
$Eu(ClO_4)_3 \cdot 7(2\text{-picNO}) \cdot 3H_2O$	−50.0	−25.0	22.0	−77.0	110.0	55.0	−1694	−55.0	−774.4	186.3
$EuCl_3 \cdot 3(2\text{-picNO}) \cdot 2H_2O$	62.7	−31.3	11.2	−83.8	145.2	72.6	−938	−72.6	−1148	136.3
$Eu(NCS)_3 \cdot 3(2\text{-picNO})$	48.7	−24.3	16.2	−92.8	153.2	76.6	−1503	−76.6	−1324	230.3
$Eu(NCS)_3 \cdot 4(2\text{-picNO})$	45.3	−22.7	15.8	−98.2	164.8	82.4	−1552	−82.4	−1513	255.7
$Eu(ReO_4)_3 \cdot 5(2\text{-picNO})$	−86.7	43.3	111.0	−51.0	−120.0	−60.0	−5661	60.0	−1286	−679.3
$Eu(ReO_4)_3 \cdot 3(2\text{-picNO})$	83.4	−41.6	108.2	−40.8	−134.8	−67.4	−4415	67.4	−1350	−595.1
$Eu(H_3C—SO_3)_3 \cdot 2(3\text{-picNO})$	66.7	−33.3	9.6	−67.4	115.6	57.8	−647	−57.8	−732.9	74.8
$Eu(NCS)_3 \cdot 3.5(3\text{-picNO})$	28.7	−14.3	−104.4	54.6	−99.6	49.8	−5700	−49.8	−1066	−567.7
$Eu(NCS)_3 \cdot 3.5(4\text{-picNO})$	65.3	−32.7	34.2	−102.8	137.2	68.6	−3516	−68.6	1293	482.4
$Eu(H_3C—SO_3)_3 \cdot 2(4\text{-picNO})$	72.7	−36.3	26.8	−84.2	114.8	57.4	−2257	−57.4	−577.8	259.1
$Eu(NCS)_3 \cdot 4pyzNO$	−71.3	35.7	82.6	−15.4	−134.4	−67.2	−1272	67.2	−1110	−171.0

$Eu(F_3C—SO_3)_3 \cdot 6pyzNO \cdot 3H_2O$	−84.0	42.0	67.2	−5.8	−122.8	−61.4	−389.8	61.4	−793.0	−47.9
$Eu(H_3C—SO_3)_3 \cdot 2pyO$	86.7	−43.3	27.0	−84.0	114.0	57.0	−2268	−57.0	−876.6	258.6
$Eu(NCS)_3 \cdot 4TMSO$	48.0	−24.0	12.6	−77.4	129.6	64.8	−975.2	−64.8	−937.3	126.4
$EuCl_3 \cdot 3TMSO$	42.6	−21.4	8.4	−71.6	126.4	63.2	−601.4	−63.2	−859.0	76.0
$Eu(NCS)_3 \cdot 3.5TMU$	−66.6	33.4	61.0	−135.0	147.0	73.0	−8235	−73.0	−1911	121.1
$EuCl_3 \cdot 4.5TSO$	57.4	−28.6	48.2	−142.8	189.2	94.6	−6883	−94.6	−2478	130.2
$Eu(NCS)_3 \cdot 5TSO$	−80.0	40.0	38.0	−104.0	132.0	66.0	−3952	−66.0	−1266	521.7
D_3 symmetry										
$Eu(H_3C—COO)_3 \cdot DMA$	−64.6	32.4	46.4	17.4	−127.6	−63.8	807.4	63.8	−733.4	1030
$EuCl_3 \cdot 3.5DMA$	−92.0	46.0	62.0	12.0	−148.0	−74.0	744	74.0	−1021	110.1
$EuCl_3 \cdot 5TMU$	−46.6	23.4	48.0	−17.0	−62.0	−31.0	−816	31.0	−273.8	−50.6
D_{3d} symmetry										
$Eu(F_3C—SO_3)_3 \cdot 7.5DMSO$	46.6	−23.4	46.0	−95.0	98.0	49.0	−4370	−49.0	−907.7	428.3
$Eu(PF_6)_3 \cdot 7.5DTMSO$	45.4	−22.6	48.6	−111.4	125.6	62.8	−5414	−62.8	−1330	680.0
$Eu(ClO_4)_3 \cdot 8pyzNO$	28.7	−14.3	35.4	−82.6	94.4	47.2	−2924	−47.2	−737.9	276.0
$Eu(PF_6)_3 \cdot 8pyzNO$	28.7	−14.3	30.2	−74.8	89.2	44.6	−2259	−44.6	−623.7	201.5
$Eu(ClO_4)_3 \cdot 7.5TMSO$	57.4	−28.6	48.4	−137.6	178.4	89.2	−6660	−89.2	−2257	1188
$Eu(PF_6)_3 \cdot 7.5TMSO$	59.4	−29.6	23.6	−92.4	137.6	68.8	−2180	−68.8	−1165	300.1
$EuBr_3 \cdot 7TMSO$	57.4	−28.6	32.2	−120.8	177.2	88.6	−3890	−88.6	−1959	689.3
$Eu(ReO_4)_3 \cdot 7.5TMSO$	47.4	−23.6	23.4	−92.6	138.4	69.2	−2167	−69.2	−1174	299.9
$EuI_3 \cdot 7.5TMSO$	62.6	−31.4	51.0	−130.0	158.0	79.0	−6630	−79.0	−1911	1048
$Eu(F_3C—SO_3)_3 \cdot 7.5TMSO$	74.6	−37.4	8.6	−95.4	173.6	86.8	−820.4	−86.8	−1589	142.4
$Eu(ClO_4)_3 \cdot 7.5TSO$	−65.4	32.6	137.4	−58.6	−157.6	−78.8	−8052	78.8	−2047	−1269
$Eu(PF_6)_3 \cdot 7.5TSO$	76.0	−38.0	56.4	−112.6	112.4	56.2	−6351	−56.2	−1267	113.8
$EuI_3 \cdot 7.5TSO$	81.3	−40.7	43.0	−127.0	168.0	84.0	−5461	−84.0	−1957	917.4
$Eu(CF_3—SO_3)_3 \cdot 7.5TSO$	40.0	−20.0	20.0	−80.0	120.0	60.0	−1600	−60.0	−880	192.0

TABLE 6
Scalar strength parameters

Complex	$^7F_1$			$^7F_2$		
	ΔE	N_v	S	ΔE	N_v	S
C_{3v} symmetry						
$Eu(ClO_4)_3 \cdot 7DMA$	75	396	65	238	1638	287
$Eu(NO_3)_3 \cdot 3DMA$	114	602	98	151	986	179
$Eu(NCS)_3 \cdot 4DMA$	75	396	65	247	1687	319
$Eu(PF_6)_3 \cdot 7DMA$	65	343	56	219	1479	272
$EuI_3 \cdot 6DMA \cdot 4H_2O$	133	703	114	264	1757	316
$Eu(NCS)_3 \cdot 4DDPA$	70	370	60	264	1827	322
$EuCl_3 \cdot 4DPPA$	186	983	160	160	1105	194
$EuBr_3 \cdot 5DPPA$	94	497	81	258	1744	320
$Eu(F_3C{-}SO_3)_3 \cdot 5DPPA$	43	227	37	306	2164	387
$EuCl_3 \cdot 3DPPM$	65	343	56	295	2049	382
$EuBr_3 \cdot 3DPPM$	117	618	101	238	1606	319
$Eu(H_3C{-}SO_3)_3 \cdot 2HMPA$	96	507	83	234	1570	289
$Eu(ClO_4)_3 \cdot 7(2\text{-picNO}) \cdot 3H_2O$	75	396	65	187	1261	227
$EuCl_3 \cdot 3(2\text{-picNO}) \cdot 2H_2O$	94	497	81	229	1572	270
$Eu(NCS)_3 \cdot 3(2\text{-picNO})$	73	386	63	246	1716	293
$Eu(NCS)_3 \cdot 4(2\text{-picNO})$	68	359	59	263	1855	313
$Eu(ReO_4)_3 \cdot 5(2\text{-picNO})$	130	687	112	231	1538	300
$Eu(ReO_4)_3 \cdot 3(2\text{-picNO})$	125	661	108	243	1609	303
$Eu(H_3C{-}SO_3)_3 \cdot 2(3\text{-picNO})$	100	528	86	183	1228	241
$Eu(NCS)_3 \cdot 3.5(3\text{-picNO})$	43	227	37	204	1436	281
$Eu(NCS)_3 \cdot 3.5(4\text{-picNO})$	98	518	85	240	1612	296
$Eu(H_3C{-}SO_3)_3 \cdot 2(4\text{-picNO})$	109	576	94	199	1314	242
$Eu(NCS)_3 \cdot 4pyzNO$	107	565	92	217	1458	257
$Eu(F_3C{-}SO_3)_3 \cdot 6pyzNO \cdot 3H_2O$	126	666	108	190	1269	240
$Eu(H_3C{-}SO_3)_3 \cdot 2pyO$	130	690	112	198	1296	240
$Eu(NCS)_3 \cdot 4TMSO$	72	380	62	207	1431	246
$EuCl_3 \cdot 3TMSO$	64	338	55	198	1387	234
$Eu(NCS)_3 \cdot 3.5TMU$	100	529	86	282	1907	368
$EuCl_3 \cdot 4.5TSO$	86	454	74	332	2291	412
$Eu(NCS)_3 \cdot 5TSO$	120	634	103	236	1563	293
D_3 symmetry						
$Eu(H_3C{-}COO)_3 \cdot DMA$	97	514	84	174	1272	208
$EuCl_3 \cdot 3.5DMA$	138	729	119	210	1470	245
$EuCl_3 \cdot 3TMU$	70	369	60	108	721	135
D_{3d} symmetry						
$Eu(F_3C{-}SO_3)_3 \cdot 7.5DMSO$	70	370	60	193	1316	257
$Eu(PF_6)_3 \cdot 7.5DTMSO$	68	359	59	237	1626	307
$Eu(ClO_4)_3 \cdot 8pyzNO$	43	227	37	177	1224	229
$Eu(PF_6)_3 \cdot 8pyzNO$	43	227	37	164	1129	209

TABLE 6 (*continued*)

Complex	$^7F_1$			$^7F_2$		
	ΔE	N_v	S	ΔE	N_v	S
$Eu(ClO_4)_3 \cdot 7.5TMSO$	86	454	74	316	2173	394
$Eu(PF_6)_3 \cdot 7.5TMSO$	89	470	77	230	1559	277
$EuBr_3 \cdot 7TMSO$	86	454	74	298	2056	361
$Eu(ReO_4)_3 \cdot 7.5TMSO$	71	375	61	231	1590	279
$EuI_3 \cdot 7.5TMSO$	94	497	81	288	1958	365
$Eu(F_3C{-}SO_3)_3 \cdot 7.5TMSO$	112	592	96	269	1857	316
$Eu(ClO_4)_3 \cdot 7.5TSO$	98	518	84	295	2007	380
$Eu(PF_6)_3 \cdot 7.5TSO$	114	602	98	225	1518	302
$EuI_3 \cdot 7.5TSO$	122	645	105	295	1979	364
$Eu(F_3C{-}SO_3)_3 \cdot 7.5TSO$	60	317	52	200	1380	241

The following relations were obtained.

$\Delta E = 0.189N_v$, $\Delta E = 1.161S$ (C_{3v} symmetry)

$\Delta E = 0.186N_v$, $\Delta E = 1.159S$ (D_3 symmetry)

and

$\Delta E = 0.146N_v$, $\Delta E = 1.162S$ (D_{3d} symmetry)

Figures 10–12 contain the N_v and S values plotted versus ΔE for the electric dipole allowed $^5D_0 \rightarrow {}^7F_2$ transitions. The equations representing the lines in the graphs and also the linear regression coefficients were calculated using the LOTUS 123 program (Lotus Development Corporation, © 1985).

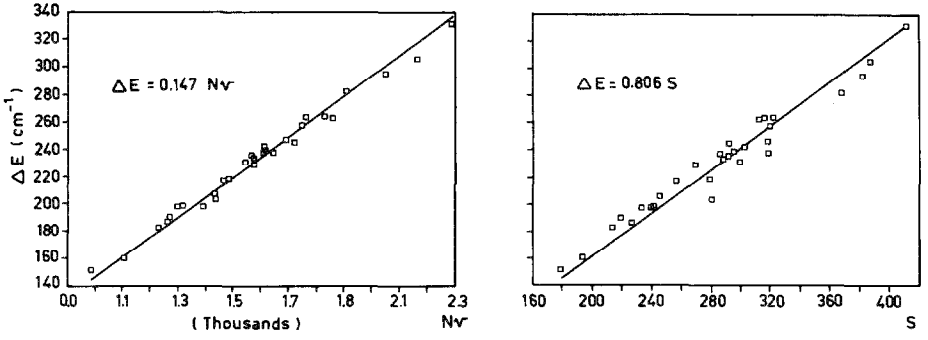

Fig. 10. Maximum Stark splitting of $^7F_2$ (Eu^{3+}) versus N_v and S in C_{3v} symmetry.

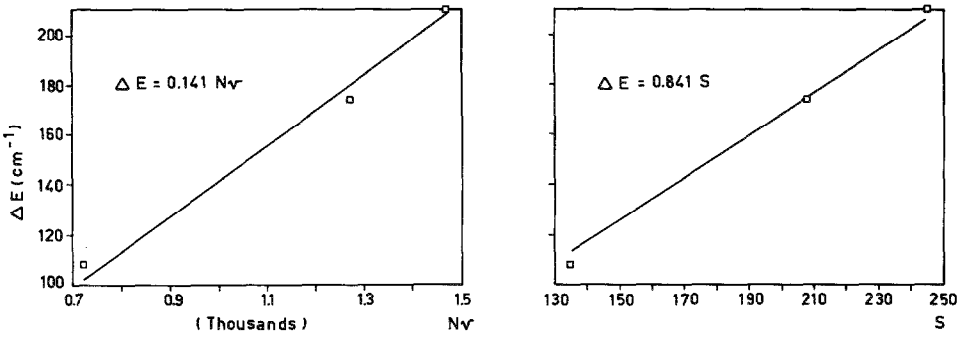

Fig. 11. Maximum Stark splitting of $^7F_2$ (Eu^{3+}) versus N_v and S in D_3 symmetry.

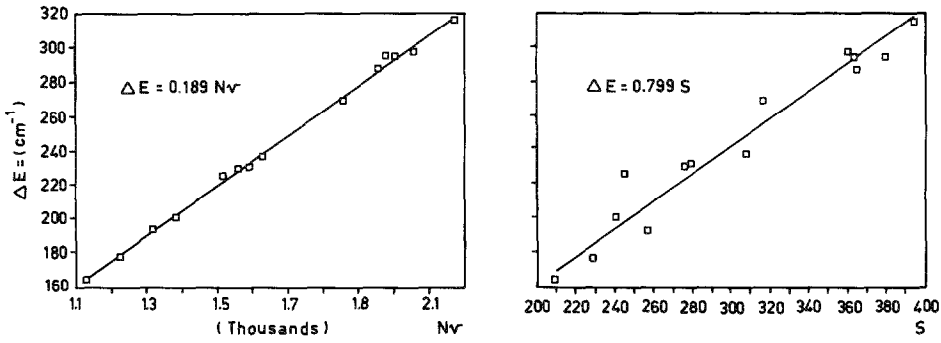

Fig. 12. Maximum Stark splitting of $^7F_2$ (Eu^{3+}) versus N_v and S in D_{3d} symmetry.

F. FINAL REMARKS

When we analyse these data, we can see that the values of N_v for the $^7F_1$ manifold are equal in modulus to $Y_2^0\langle r^2\rangle$ for all three symmetries.

Comparing the N_v and S values of the $^7F_2$ manifold in an attempt to establish a spectrochemical series of the ligands based on the crystal-field splitting, it was observed that

(a) taking the N_v and ΔE values for all compounds containing NCS^- as counter-ion, with C_{3v} symmetry, the splitting of the levels follows the order:

TMU > 2-picNO (CN = 7) > DDPA > 2-picNO (CN = 6)
> DMA > 4-picNO > TSO > pyzNO > 3-picNO > TMSO

(b) using S and ΔE for the same compounds, a different order, with some inversion, was obtained:

TMU > DDPA > DMA > 2-picNO (CN = 7) > 4-picNO > 2-picNO (CN = 6)
= TSO > 3-picNO > pyzNO > TMSO

(c) using compounds containing Cl^- as counter-ion, the order is the same for N_v and S:

TSO > DPPM > 3-picNO + H_2O > TMSO > DPPA

(d) using $H_3C–SO_3^-$ as counter-ion, the order for both parameters is:

HMPA > 4-picNO > 3-picNO > pyO

(e) in the case of compounds with D_{3d} symmetry with TMSO as ligand and the same apparent coordination number and using N_v and S parameters, the anions, despite the fact that they are not directly coordinated to the central ion due to their basicity, influence the splitting as:

$ClO_4^- > I^- > CF_3SO_3^- > ReO_4^- > PF_6^-$

(f) with TSO as ligand, an inversion in order is observed:

$ClO_4^- > I^- > PF_6^- > CF_3SO_3^-$

(g) with pyzNO as ligand

$ClO_4^- > PF_6^-$

(h) in general, the following order is observed when the same counter-ion, the same symmetry (D_{3d}) and the same coordination number is used

TMSO > TSO > pyzNO

The scalar parameters S were plotted in relation to N_v for the three symmetries under consideration. A reasonable correlation was obtained in all cases, indicating that these parameters are both consistent and reflect the same trends.

To correlate the splittings with chemical properties of the different ligands is not an easy task since we may have different coordination numbers, the structures are not known, and the ligands have different basicities, geometries and bulkiness. Nevertheless, the bonding is essentially electrostatic and it is possible to conclude that basicity is the predominant factor.

ACKNOWLEDGEMENTS

One of us (M.C.F.C.) acknowledges a Ph.D fellowship from Conselho Nacional de Desenvolvimento Científico e Tecnológico (CNPq). The authors are much indebted to CNPq and Fundação de Amparo à Pesquisa do Estado de São Paulo (FAPESP) for financial support.

REFERENCES

1 B.G. Wybourne, Spectroscopic Properties of Rare Earths, Interscience, New York, 1965.
2 C.A. Morrison and R.P. Leavitt, In K.A. Gschneidner, Jr. and L. Eyring (Eds.), Handbook on the Physics and Chemistry of Rare Earths, Vol. 5, North-Holland, Amsterdam, 1982, p. 461.
3 K.W.H. Stevens, Proc. Phys. Soc. London Sect. A, 65 (1952) 209.
4 R.J. Elliot and K.W.H. Stevens, Proc. Phys. Soc. London Sect. A, 218 (1953) 553.
5 M.T. Hutchings, Solid State Phys., 16 (1964) 227.
6 A. Lempicki, H. Samelson and C. Brecher, J. Mol. Spectrosc., 27 (1968) 375.
7 J.L. Prather, Atomic Energy Levels in Crystals, Monograph 19, National Bureau of Standards, Washington, DC, 1961.
8 F. Auzel and O.L. Malta, J. Phys., 44 (1983) 201.
9 R.P. Leavitt, J. Chem. Phys., 77 (1982) 1661.
10 N.C. Chang, J.B. Gruber, R.P. Leavitt and C.A. Morrison, J. Chem. Phys., 76 (1982) 3877.
11 R.P. Leavitt, J.B. Gruber, N.C. Chang and C.A. Morrison, J. Chem. Phys., 76 (1982) 4775.
12 Y.Y. Yeung and D.J. Newman, J. Chem. Phys., 82 (1985) 3747.
13 Y.Y. Yeung and D.J. Newman, J. Chem. Phys., 84 (1986) 4470.
14 D.E. Henrie and G.R. Choppin, J. Chem. Phys., 49 (1968) 477.
15 S.P. Sinha, Spectrochim. Acta, 22 (1966) 57.
16 T. Moeller and G. Vicentini, J. Inorg. Nucl. Chem., 27 (1965) 1477.
17 G. Vicentini and E. Carvalho, Jr., J. Inorg. Nucl. Chem., 28 (1966) 2987.
18 G. Vicentini and J.C. Prado, Cienc. Cult., 19 (1967) 687.
19 G. Vicentini and R. Najjar, J. Inorg. Nucl. Chem., 30 (1968) 2771.
20 G. Vicentini, R. Najjar and C. Airold, An. Acad. Bras. Cienc., 41 (1969) 375.
21 G. Vicentini and L.R.F. Carvalho, J. Inorg. Nucl. Chem., 39 (1977) 540.
22 G. Vicentini, L.B. Zinner and K. Zinner, Rev. Latinoam. Quim., 10 (1979) 90.
23 G. Vicentini, L.B. Zinner, A.M.P. Felicissimo and K. Zinner, J. Inorg. Nucl. Chem., 41 (1979) 1611.
24 L.B. Zinner and G. Vicentini, An. Acad. Bras. Cienc., 58 (1986) 183.
25 G. Vicentini, L.B. Zinner and L. Rothschild, Inorg. Chim. Acta, 9 (1974) 213.
26 L.R.F. Carvalho and G. Vicentini, J. Coord. Chem., 11 (1981) 67.
27 G. Vicentini and J.C. Prado, J. Inorg. Nucl. Chem., 34 (1972) 1309.
28 G. Vicentini and M.A. Silva, Rev. Latinoam. Quim., 12 (1981) 24.
29 L.R.F. Carvalho, G. Vicentini and K. Zinner, J. Inorg. Nucl. Chem., 43 (1981) 1088.
30 A.B. Nascimento, G. Vicentini, L.B. Zinner and H.F. Brito, Lanthanide Actinide Res., 2 (1988) 253.
31 G. Vicentini, L.B. Zinner and G. Lüders Neto, in, G. Vicentini and L.B. Zinner (Eds.), Anais do X-Simpósio Anual da Academia de Ciências do Estado de São Paulo, Vol. I, Química dos Lantanídeos e Actinídeos, 1986, p. 131.
32 G. Vicentini and J.E. Viana, An. Acad. Bras. Cienc., 48 (1976) 709.
33 G. Vicentini and L.R.F. Carvalho, in G.J. McCarthy, H.B. Silber and J.J. Rhyne (Eds.), Rare Earths in Modern Science and Technology, Plenum Press, New York, 1982, p. 213.
34 G. Vicentini and G. Chiericato, Jr., An. Acad. Bras. Cienc., 51 (1979) 217.
35 A.M.P. Felicissimo, G. Vicentini and L.B. Zinner, An. Acad. Bras. Cienc., 54 (1982) 65.
36 L.B. Zinner and A.M.P. Felicissimo, An. Acad. Bras. Cienc., 49 (1977) 139.
37 A.M.P. Felicissimo and L.B. Zinner, An. Acad. Bras. Cienc., 49 (1977) 537.
38 A.M.P. Felicissimo, L.B. Zinner, G. Vicentini and K. Zinner, J. Inorg. Nucl. Chem., 40 (1978) 2067.

39 L.B. Zinner and G. Vicentini, An. Acad. Bras. Cienc., 51 (1979) 443.
40 L.B. Zinner, G. Vicentini and A.M.P. Felicissimo, Rev. Latinoam. Quim., 11 (1980) 65.
41 L.B. Zinner, J.R. Matos and A.B. Nascimento, Inorg. Chim. Acta, 141 (1988) 305.
42 G. Vicentini, M.C. França da Cunha and L.B. Zinner, J. Less Common Met., 149 (1989) 255.
43 G. Vicentini, M.C.F. Cunha and L.B. Zinner, Eur. J. Solid State Inorg. Chem., 28 (1991) 279.
44 L.B. Zinner and J.R. Matos, Eur. J. Solid State Inorg. Chem., 28 (1991) 295.
45 G. Vicentini and L.B. Zinner, Inorg. Nucl. Chem. Lett., 10 (1974) 629.
46 L.B. Zinner and G. Vicentini, J. Inorg. Nucl. Chem., 37 (1975) 1999.
47 G. Vicentini, L.B. Zinner and M.A. Silva, An. Acad. Bras. Cienc., 52 (1980) 23.
48 G. Vicentini, L.B. Zinner, O.J. Fentanes and M.A. Silva, An. Farm. Quim. São Paulo, 20 (1980) 181.
49 G. Vicentini and M.A. Silva, An Acad. Bras. Cienc., 54 (1982) 71.
50 L.B. Zinner and J.R. Matos, Lanthanide Actinide Res., 3 (1990) 195.
51 L.B. Zinner and G. Vicentini, Inorg. Nucl. Chem. Lett., 7 (1971) 967.
52 L.B. Zinner and G. Vicentini, An. Acad. Bras. Cienc., 45 (1973) 223.
53 G. Vicentini, L.B. Zinner and L. Rothschild, An. Acad. Bras. Cienc., 45 (1973) 353.
54 G. Vicentini, L.B. Zinner and L.R.F. Carvalho, J. Inorg. Nucl. Chem., 37 (1975) 607.
55 G. Vicentini and A.M.S. Vieira, An. Acad. Bras. Cienc., 48 (1976) 725.
56 G. Vicentini, K. Umeda and I. Giolito, An. Acad. Bras. Cienc., 49 (1977) 143.
57 L.B. Zinner and G. Vicentini, in G.J. McCarthy and J.J. Rhyne (Eds.), Rare Earths in Modern Science and Technology, Plenum Press, New York, 1978, p. 155.
58 L.B. Zinner and F.A. Araújo, in G.J. McCarthy, H.B. Silber and J.J. Rhyne (Eds.), Rare Earths in Modern Science and Technology, Plenum Press, New York, 1982, p. 217.
59 L.R.F. Carvalho, An. Acad. Bras. Cienc., 54 (1982) 649.
60 M. Perrier, R. Najjar and G. Vicentini, An. Acad. Bras. Cienc., 42 (1970) 439.
61 M. Perrier and G. Vicentini, J. Inorg. Nucl. Chem., 35 (1973) 555.
62 H.F. Brito, Ph.D. Thesis, University of São Paulo, 1988.
63 G. Vicentini and L.C. Garla, J. Inorg. Nucl. Chem., 35 (1973) 3973.
64 G. Vicentini and A.M.S. Vieira, An. Acad. Bras. Cienc., 45 (1973) 371.
65 G. Vicentini and M. Perrier, J. Inorg. Nucl. Chem., 36 (1974) 77.
66 G. Vicentini, L.B. Zinner and L.R.F. Carvalho, An. Acad. Bras. Cienc., 47 (1975) 87.
67 G. Vicentini, L.B. Zinner and K. Zinner, J. Inorg. Nucl. Chem., 40 (1978) 690.
68 A.M.P. Felicissimo, G. Vicentini, L.B. Zinner and Y. Shimizu, An. Acad. Bras. Cienc., 52 (1980) 283.
69 G. Vicentini, L.B. Zinner, A. Oliveira da Silva and P.O. Dunstan, Lanthanide Actinide Res., 1 (1985) 143.
70 G.H. Dieke, Spectra and Energy Levels of Rare Earth Ions in Crystals, Interscience, New York, 1968.
71 S. Hüfner, Optical Spectra of Transparent Rare Earth Compounds, Academic Press, New York, 1978.
72 Z.N. Goldschmidt, in K.A. Gschneidner and L. Eyring (Eds.), Handbook of the Physics and Chemistry of Rare Earths, Vol. 1, North-Holland, Amsterdam, 1978, p. 1.
73 C.K. Jørgensen, Absorption Spectra and Chemical Bonding in Complexes, Pergamon, London, 1962.
74 B.R. Judd, Operator Techniques in Atomic Spectroscopy, McGraw-Hill, New York, 1963.
75 E.V. Condon and G.H. Shortley, The Theory of Atomic Spectra, Cambridge University Press, London, 1959.

76 I.I. Sobelman, Atomic Spectra and Radiative Transitions, Springer-Verlag, Berlin, 1979.
77 G. Racah, Phys. Rev., 62 (1942) 438; 63 (1943) 367; 76 (1949) 1352.
78 C.W. Nielson and G.F. Koster, Spectroscopic Coefficients for p^n, d^n and f^n configurations, MIT Press, Cambridge, MA, 1964.
79 B.G. Wybourne, Symmetry Principles and Atomic Spectroscopy, Wiley-Interscience, New York, 1969.
80 A.B. Nascimento and G. Vicentini, in G. Vicentini and L.B. Zinner (Eds.), Anais do VIII-Simpósio Anual da Academia de Ciências do Estado de São Paulo, Vol. 1, Química das Terras Raras, 1984, p. 185.
81 A.B. Nascimento, G. Vicentini and L.B. Zinner, An. Assoc. Bras. Quim., 38/39 (1–4) (1987–1988) 53.
82 N. Rotenberg, R. Bivins, N. Metropolis and J.K. Wooten, The 3-j and 6-j Symbols, Technology Press, Cambridge, 1959.
83 Landolt-Börnstein, Numerical Data and Functional Relationships in Science and Technology, Springer-Verlag, Berlin, 1968.
84 A. Abragan and B. Bleaney, Electron Paramagnetic Resonance of Transitions Ions, Oxford University Press, London, 1970.
85 P. Porcher, M.Sc. Thesis, Paris VI, 1977.
86 A.B.P. Lever, Inorganic Electronic Spectroscopy, Elsevier, Amsterdam, 1968.
87 J.H. Forsberg, Coord. Chem. Rev., 10 (1973) 195.
88 P. Porcher and P. Caro, J. Lumin., 21 (1980) 207.
89 B.E. Douglas and C.A. Hollingsworth, Symmetry in Bonding and Spectra. An Introduction, Academic Press, London, 1985.
90 G.F. Koster, J.O. Dimock, R.G. Wheeler and H. Statz, Properties of Thirty Two Point Groups, MIT Press, Cambridge, MA, 1963.
91 A.B.P. Lever, Inorganic Electronic Spectroscopy, Elsevier, Amsterdam, 2nd edn., 1984.
92 G. Vicentini, M.C.F. Cunha and L.B. Zinner, J. Less Common Met., 149 (1989) 255.
93 A.B. Nascimento, G. Vicentini, L.B. Zinner and H.F. Brito, Lanthanide Actinide Res., 2 (1987) 253.
94 A.J. Kassman, J. Chem. Phys., 53 (1970) 118.